2015 IEEE/RSJ International Conference on Intelligent Robots and Systems (IROS)
Congress Center Hamburg
Sept 28 - Oct 2, 2015. Hamburg, Germany

Design of Mesoscale Active Cells for Networked, Compliant Robotic Structures

Ahsan I. Nawroj, *Student Member, IEEE,* John P. Swensen, *Member, IEEE*, and Aaron M. Dollar, *Senior Member, IEEE*

Abstract— **We present the design of simple, centimeter-scale modular actuation units ("Active Cells") and passive compliant nodes that are electromechanically networked to create macroscopically deformable Modular Active Cell-based Structures (MACROs). Each Active Cell is a single degree-of-freedom linear actuator (a "muscle unit"), consisting of fiberglass end-pieces connecting two strands of Nitinol shape-memory alloy and a passive biasing spring. The Nitinol strands are coiled into a tight spring to increase deformations when activated through resistive heating. In-depth examination of the optimization of Nitinol coils with an antagonistic spring is presented, resulting in large repeatable axial cell strains of up to 25%. The design of these cellular muscle units to obtain maximal repeatable stroke is presented, allowing for the construction of larger networks of cells (MACRO modules, akin to a biological "tissue") that can be customized to a target application. Finally, experimental demonstration of the construction and actuation of some simple MACRO modules is described.**

I. INTRODUCTION

A large amount of research exists in modular and reconfigurable robots (e.g. [1]–[4]), the majority of which relies on "units" that are self-contained robots themselves, complete with their own suite of actuators (generally for mobility), sensors, power source, and control electronics, resulting in systems with fundamental lower limits on the sizes that can be achieved, as well as practical difficulties for fabrication in large numbers. Alternatively, we are working towards a much simpler concept of electromechanical units that we call 'active cells' (Figure 1), which can be connected in a network using compliant nodes to create Modular Active Cell-based Robots (MACROs). Active cells are inspired by biological systems where multicellular organisms comprise groups of specialized cells that together form complex systems. Such complex structures found in nature (akin to the proposed MACRO modules) use groups of relatively simple cells working in concert to create large swaths of highly articulable macroscopic tissues. Specific examples of such functional structures include muscles lining the

This work was supported in part by the National Science Foundation grants IIS-1317976 and the Air Force Office of Scientific Research grant FA9550-11-1-0093.

A.I. Nawroj, J.P. Swensen, and A. M. Dollar are with the Department of Mechanical Engineering and Materials Science, Yale University, New Haven, CT, USA. (e-mail: {ahsan.nawroj; john.swensen; aaron.dollar}@yale.edu)

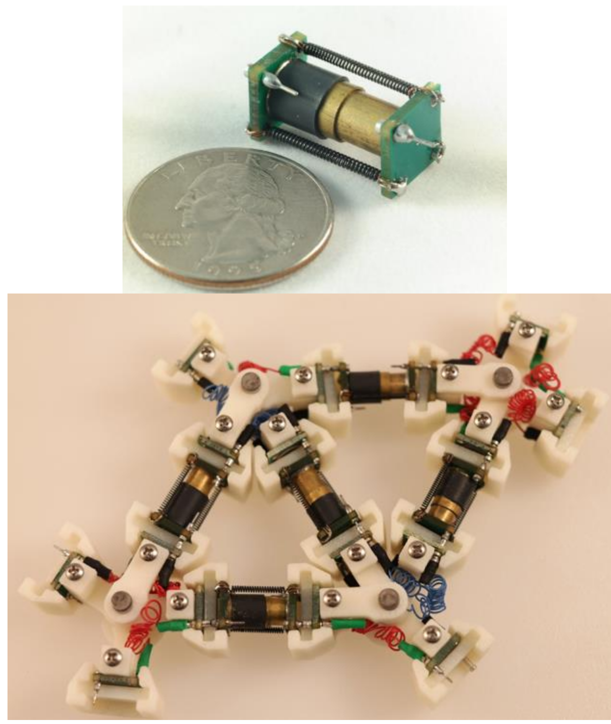

Figure 1 Active Cell v2.0 (top). A sample MACRO module made using Active Cells and Nodes (bottom).

gastrointestinal tract capable of anterograde waves of peristaltic motion [5], cardiac muscle that operates with rhythmic cellular activation [6], and many others. A careful look at a complex tissue such as the human heart shows the principal action of the structure comes from myocardiocytes that are simultaneously structural and contractile. The high degree of mobility of the entire structure occurs through planned stimulation of the myocardiocytes by nearby pacemaker cells.

Nearly all existing approaches to modular robots can be classified as either being very general-purpose (with the attendant complexity) or simple, mostly passive components. There have been a number of impressive projects involving highly capable general purpose modular robots, including CKBots [7] and SMORES [8]. Much of the theoretical consideration for modular and cellular robotics was presented by Fukuda and Ueyama [9], which parlays into the expanding field of cooperative and distributed robotics (e.g. [10], [11]). Thorough reviews of the work in the area prior to 2009 are found in [12], [13]. On the spectrum of the simpler modular robot projects, roBlocks [14] (later commercialized as Cubelets by Modular Robotics LLC), are single-function blocks but are not particularly simple in terms of design. A related approach to simple, crystalline robots that achieved volume change through linear actuators in all directions was developed by Rus and Vona [15]. An important related inspiration is in the study of variable geometry trusses and adaptive structures, which explore much of the structural theory our work uses for robotics [16], [17]. More recent work more closely related to our approach has been the encasing of a Nitinol braid into a tube or solid sphere [18] and the creation of a cellular material where the pressure in each chamber affects the bulk material properties [19].

Our work is differentiated from this body of existing work by the simplicity of the cells we have fabricated and their scalability in size and actuation method. We have previously engineered [20], [21] a rapidly prototyped cell that used NiTi SMA (Nickel-Titanium Shape-Memory Alloy) as the contractile element in the form of coils, connecting plastic plates that provide an interface for connection and power transmission. Resistive heating from an off-board power signal flowing through the shape-memory alloy activates the cells. Despite thermodynamic inefficiencies and low bandwidth of operation, Nitinol Shape-memory alloy has better achievable strain and durability than other material actuators [22]. Material actuators are generally desirable due to their potential to be utilized at very small scale, simple powering schemes (Joule heating for Nitinol), and lack of required complicated complementary structures (Lorentz force actuators, for example, require bearings, magnets, and a physical/electronic means of commutation between coils).

In this paper we begin with a description of the proposed complaint Modular Active Cell-based Robots (Section II). We describe the design of Active Cells that constitute the actuators for MACROs using a SMA actuation model we develop from experimental data and subsequent design optimizations of cell stroke using this model of SMA and passive springs (Section III). Next we describe the design of inter-cell connection mechanisms that function as nodes in complex n-degree networks of our robots (Section IV). We use Active Cells and passive nodes to construct prototype MACRO modules, demonstrating the feasibility of using our designs for realizable cellular robots (Section V). We finish with a discussion of the contributions and limitations of our current approach and identify future work (Section VI).

II. Compliant Structural Robot

Our proposed compliant Modular Active-Cell based Robots (MACROs) consists of articulated links connected by passive nodes in a homogeneous mesh. The links are what we call Active Cells, which are simple contractile actuation elements. MACROs are designed to be inherently modular, with multiple smaller Active-Cell networks (smaller MACROs) combining to create larger, more functional modules. MACROs have a high number of degrees-of-freedom and can be locally controlled by the application of power to the nodes. A diagram of a small MACRO module and its proposed operation is shown on Figure 2. An exploded view of the Active Cells that constitute a MACRO is shown on Figure 3.

The following sections describe the design of the components of the MACRO modules, culminating in some

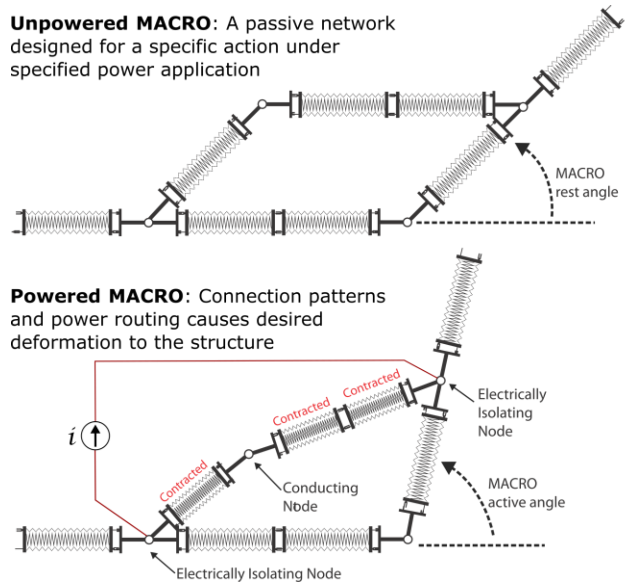

Figure 2 Diagram showing Modular Active-Cell based Robotic (MACRO) module (top), and the deformations to the module structure when activated (bottom).

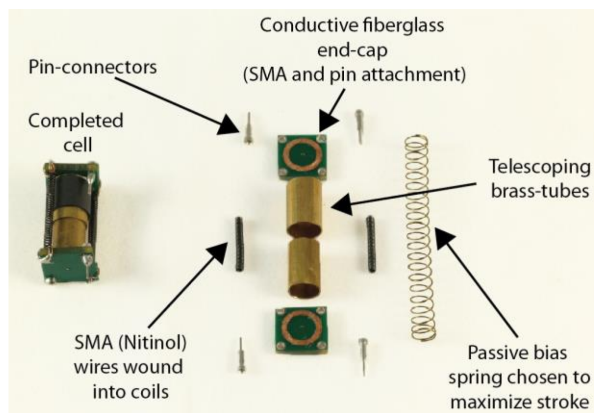

Figure 3 Active Cell v2.0 exploded view (completed cell on the left).

simple prototyped MACROs. We leave descriptions of the control schema to achieve fully-specified target deformations in the structure for future work.

III. Design of Active Cells

A. Cell Design Specifications and Parameters

Our previous work in this area [21] described the design of a rapidly prototyped actuator cell design with printed plastic end-caps to provide connectivity to adjacent cells. These initial cell designs (Cell v1.0) measured 25mm x 25mm in its cross-section and approximately 31mm in length. When fully contracted, the cell was 26mm in length, providing a recoverable strain of ~15.4%. We followed the initial design with several design iterations to decrease the cell size and obtain better strain performance. A diagram showing the cell design is shown on Figure 4. The improved design (Cell v2.0, features a size of 10mm x 10mm cross section and a rest length of 18.7 mm. Fully contracted cells are 14.4 mm long, providing a recoverable strain of 23.0%. Along with this ~50% increase in strain, Cell v2.0 contains fewer parts than its predecessor, containing a single channel of power routed through two NiTi (Nickel-Titanium Shape Memory Alloy) coils. Relevant mechanical and electrical properties of the latest cell iteration are provided in Table 1.

The design parameters of the Active Cell we modified to improve the stroke of the cell are the geometry of the SMA coils and passive spring. We chose to only alter the length of the SMA coil ($l_{0\text{-}SMA}$) and set the wire and coil diameters to a fixed known value. Both the spring rest length ($l_{0\text{-}Spring}$) and rate (k_{Spring}) were varied during design optimization. The physical properties of the SMA coil was kept constant by standardizing the fabrication process: all coils are made from 0.305 mm (diameter d) SMA wire wound around a 1 mm (diameter D) piano wire with memory shapes set at 450ºC for 15 minutes. SMA properties are strongly affected by the annealing process, and we used results from [23] to use a process (annealing temperature and time) that minimizes detwinning force and permanent plastic deformation in the coils over repeated trials. The values of the design parameters $l_{0\text{-}SMA}$, $l_{0\text{-}Spring}$, and k_{Spring} were determined through a design optimization process that maximizes cell stroke (described in the following subsections).

B. SMA Actuation Model

NiTi shape memory alloys actuate using a phase change phenomenon from a detwinned martensitic lattice to the more compact austenitic lattice when heat is applied. Unloaded

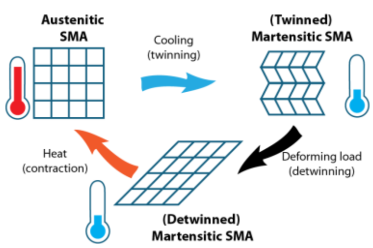

Figure 5 Diagram of SMA Activation cycle.

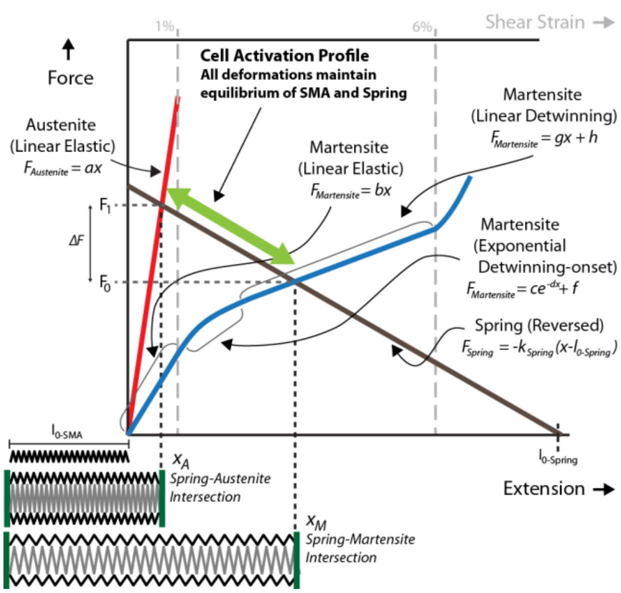

Figure 6 A typical SMA force deflection profile in the presence of a biasing spring. Note the SMA profile would alter with geometry of the coils, material properties of the SMA. The biasing spring affects the effective stroke of the combined mechanism as the spring stiffness and rest length is varied. Equations shown on the figure constitute our parametrized model of the SMA coils, and are described in the text.

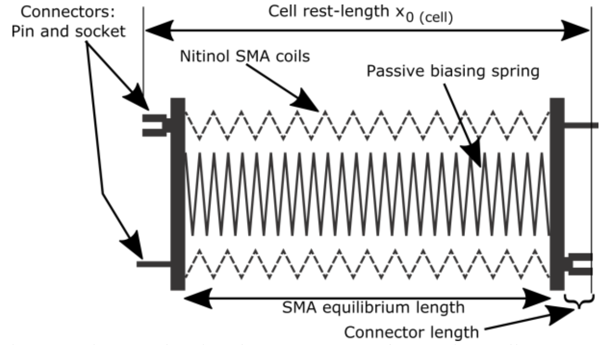

Figure 4 Diagram showing the components of an Active Cell

Cell Property	Value	
Cell rest length	18.7 +/- 0.6 mm	
Square cross-section dimension	10.2 mm	
Rest length of Nitinol coils	9.05 mm	
Coil diameter	1.305 mm	
Nitinol wire diameter	0.305 mm	
Bias-spring rest length	35 mm	
$\mathbf{k_{Spring}}$	0.142 N/mm	
Overall cell stroke	4.3 +/- 0.6 mm (19.7-26.2%)	
Overall cell resistance	0.8 ohms	
Activation temperatures	$T_{Austenite\text{-}Start}$	40°C
	$T_{Austenite\text{-}Finish}$	50°C
	$T_{Martensite\text{-}Start}$	45°C
	$T_{Martensite\text{-}Finish}$	25°C

Table 1 Mechanical and Electrical properties of Active Cells.

SMA cycled through austenitic phase cooled below the austenite-start temperature is in twinned martensitic structure. Applied loads detwin the martensite, and the shape is recovered upon heating (Figure 5). Commercial NiTi SMAs recommend limiting shear strains in the material of to 6% for repeatable, non-deteriorating phase-transition cycling. Our design of Active Cells use helically wound SMA wire into active springs, and we constrain the cell design to induce no larger than 6% shear strain in the SMA. Additionally, since SMA is a unidirectional actuator – an external restoring stress must be applied to strain it to its detwinned state – we chose a passive linear spring to apply this detwinning stress.

NiTi SMA actuators have been used as straight drawn wires ([24], [25]) and as helically wound coils ([26][27]) in a variety of robotic applications. Most authors treat the coiled NiTi SMA with mechanical spring equations with two different shear moduli, G_M and G_A for martensite and austenite lattice behavior respectively. As Figure 6 shows, however, the strain response of martensitic SMA is highly nonlinear and there is a notable change in free-length of the spring during operation. A linear spring model is only valid for a short percentage strain of the martensitic SMA coil and not accurate for high shear strains. To better capture the nonlinearity of the force-deflection curves of SMA in its two states, we collected experimental data for several lengths of coils (force vs. extension, using an Instron [28] tensile tester) and used a new pair of parametrized fitting functions to model the profiles. For coils with diameter D made from wires of diameter d (Table 1), and n loops of wire, we modeled austenitic coils (temperature $T > T_{Austenite\text{-}Finish}$) having profiles of force (F) and deflection from rest-length (x) (for parameter a) as

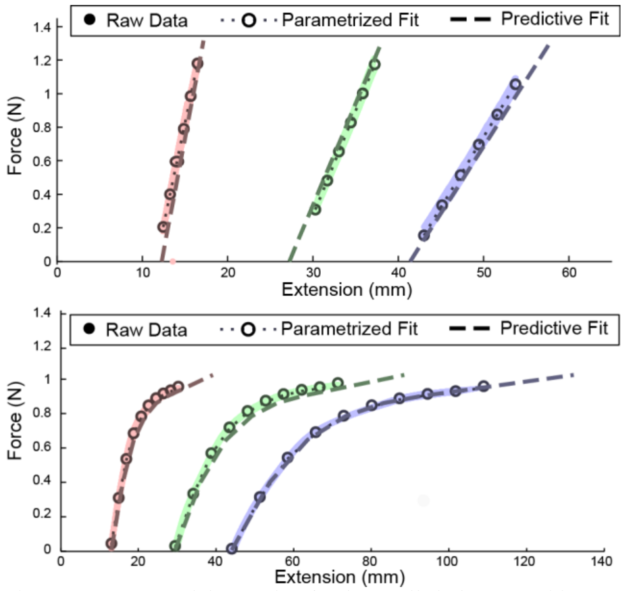

Figure 7 Force vs. axial extension for three coils in hot austenitic state (top) and cold martensitic state (bottom). Experimental data is shown in faded colored dots. Linear model fit for each coils is shown in dotted-circles. Predicted profiles from scaling laws and mean parameters are shown in dashed lines.

$$F_{Austenite}(x) = ax \tag{1}$$

For the same coils in martensitic state ($T < T_{Martensite\text{-}Start}$), we modeled the force-deflection using a three piece function consisting of a linear elastic region, an exponential onset of detwinning and a linear detwinning region (for parameters *b, c, d, f, g, h,* x_1 and x_2) as

$$F_{Martensite}(x) = \begin{cases} bx & x \leq x_1 \\ ce^{-dx} + f & x_1 < x \leq x_2 \\ gx + h & x > x_2 \end{cases} \tag{2}$$

Using least-squares minimization over experimentally collected data, we obtained parameter values for the stated constants. The experimental data and their fits are shown on Figure 7. Cho et al. [29] provide a set of equations derived from coil geometry to relate force and deflection to shear-stress and shear-strain in the coils, and these normalized shear-stress vs. shear-strain curves of varying coil geometry are identical. This normalization suggests that the force-deflection profiles of the coils are essentially identical within scale, and this is verified by using the parameters for one of the coils and rescaling them by the length ratio of the coils using. Thus, for a coil of length l, the force-deflection profile (for either material state) can be written in terms of the parameters for a known length l_0, leveraging this linearity, as

$$F\,(l_1) = \left({}^{l_1}/_{l_0}\right) F(l_0). \tag{3}$$

Although it is sufficient from a design perspective to obtain a predictive fit within scale, we note that the fitting piecewise functions can be related to material properties and geometry of the coils. This is evident while relating the SMA shear moduli G_A and G_M from the linear regimes of the force deflection profiles, and can be computed from

$$G_A = a\frac{8D^3n}{d^4}, G_M = b\frac{8D^3n}{d^4} \tag{4}$$

Extensions to this modeling work will relate the remaining fitting parameters to material and geometric properties, in the spirit of [29], [30]. The relevant equations for this paper are simply the scaling laws stated earlier, which allows us to predict changes in behavior as coil geometry is varied.

C. *Design Optimization for Cell Stroke*

From Figure 6 and the parametrized equations described in the last section, the stroke of the cell can be written as

$$x_{stroke} = x_M - x_A \tag{5}$$

$$\begin{aligned} x_M &= \{x: F_{Martensite}(x, l_{0_{SMA}}) = F_{Spring}(x)\} \\ x_A &= \{x: F_{Austenite}(x, l_{0_{SMA}}) = F_{Spring}(x)\} \end{aligned} \tag{6}$$

The $F_{Martensite}$ and $F_{Austenite}$ functions are the parametrized equations scaled appropriately as the length of the SMA coils is changed. The spring equation (adjusted for biasing attachment) is

$$F_{Spring}(x) = -k_{Spring}(x - l_{0_{Spring}}) \tag{7}$$

Using the definition of stroke, we set up a constrained optimization problem as follows:

$$\begin{Bmatrix} l^*_{0_{SMA}} \\ k^*_{Spring} \\ l^*_{0_{Spring}} \end{Bmatrix} = \underset{\{l_{0_{SMA}},\, k_{Spring},\, l_{0_{Spring}}\}}{argmax} (x_M - x_A) \tag{8}$$

$$\gamma_{x_A} \leq 0.01, \qquad \gamma_{x_M} \leq 0.06 \tag{9}$$

$$l_{0_{Spring}} \leq l_{Spring-Max} \tag{10}$$

The shear-strains (γ) induced in the coils at the points x_M and x_A are computed using equations from [29].

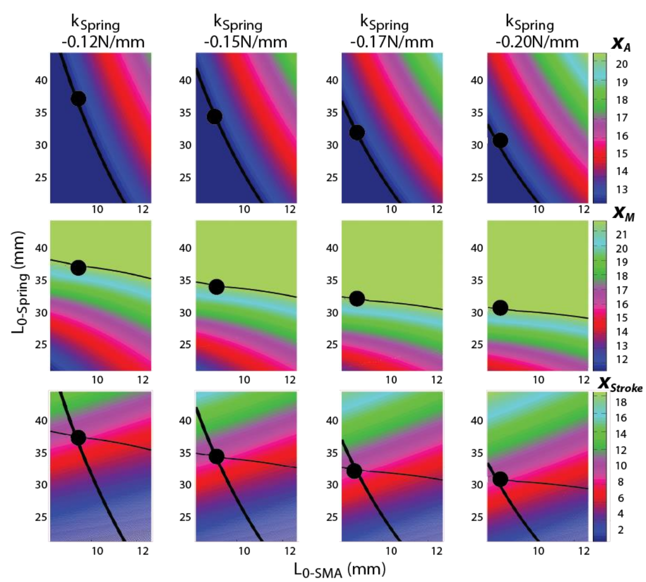

Figure 8 Two of the constraint functions used in the optimization: x_A (top row), x_M (middle row) shown as a function of the spring and SMA lengths and discretized spring rates. The computed stroke (bottom row) is a smooth function of the parameters. The optimal selection of the parameters is shown as a black circle. Four sample values of the discretized spring rate is shown (80%, 100%, 120%, 140% of the optimal k^*_{Spring}). Note the constraint limits of the top two plots is plotted on the objective function (stroke) to show that the optima lies on one of the vertices of the constraint polygon.

Node Property	Rigid-Arm
Arm length	20.65 mm
Cell-attachment mechanism	Pins mate to Cell connector
Maximum angular range (4-arm)	34 degrees
Node stiffness (attached springs)	0.16 N/mm
Maximum force for full deflection	0.97 N

Table 2 Mechanical properties of Nodes.

A plot showing the effect of the three design parameters on the computed cell stroke is shown on Figure 8. The constrained maximization of stroke provides the optimal choice of these parameters (used in the latest cell). Given these optimal parameter values ($l_{0\text{-}SMA}^* = 9.05mm$, $l_{0\text{-}Spring}^* = 35.0mm$, and $k_{Spring}^*=0.142\ N/mm$), the expected tensile force exerted by the cell can be calculated to be $\Delta F = 1.3$ N (marked on Figure 6).

IV. Design of Passive Nodes

We designed the passive nodes of the MACRO networks as compliant revolute joints, realizable with rigid links and springs or as flexural pivots. Examples of rigid-arm node prototypes are shown on Figure 9.

Rigid nodes are simpler to fabricate and customize, but they contain a larger number of parts with non-trivial friction between moving components, and it is difficult to scale down rapidly prototyped components (note the large size of the examples provided in Figure 9). The modification of inter-arm compliance is, however, considerably easier in rigid nodes, as it involves inserting any number of elastic bands of known stiffness on the holding screws above each arm. Alternatively, flexure-based nodes are monolithic with no friction between arms, and can be fabricated to considerably smaller dimensions. However, adjusting compliance between arms of the node involves completely remolding the node with different flexure-pivot geometry. Rigid-arm node dimensions and properties used in this paper are shown on Table 2. Comparison between different node designs, reduction in overall size of nodes, material used in node fabrication, and the optimization of node geometry to improve performance of networked cells is left for future work.

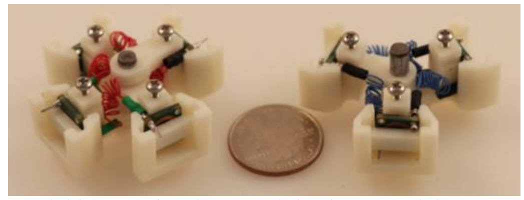

Figure 9 Rigid-arm nodes: degree-4 (left), degree-3 (right). Compliance between arms in the rigid node can be adjusted by attaching elastic bands or extension springs between the screws mounted on each arm.

V. Prototype MACRO Modules

Using our collection of fabricated Active Cells (15 to date) and the rigid-arm nodes, we prototyped several simple two-dimensional structures. These structures serve as proof-of-concept for the MACRO modules described earlier. Several of these structures in their assembled shape as well as the deformed shape (once the marked cells are activated by electric power) are shown on Figure 10. The nodes were powered with a constant-current power source at a current to drive 1.5A through the marked cells on Figure 10 for 5s. An important consideration during operation of any MACRO is the cooling system. For these prototypes, we allowed environmental cooling within identical test setups. Future work will explore control of cooling conditions to affect the operational bandwidth of the MACRO. It is worth noting that due to the properties of SMA, the MACRO modules cannot be high bandwidth systems, but significant changes to the intrinsic rate of deformation (~5s for 1.5A through a cell) can be made using appropriate current control and cooling systems. Additionally, note that the rigid-arm nodes are considerably larger than Active Cells, and thus relative deformations to the structure are minimal with each link in the network being of length 1 cell. Figure 10 shows a preliminary potential to create controllable deformations in a networked structure using the Active Cells and nodes. In order to cause larger shape deformations, we intend to study the design of smaller nodes (akin to the flexure-nodes

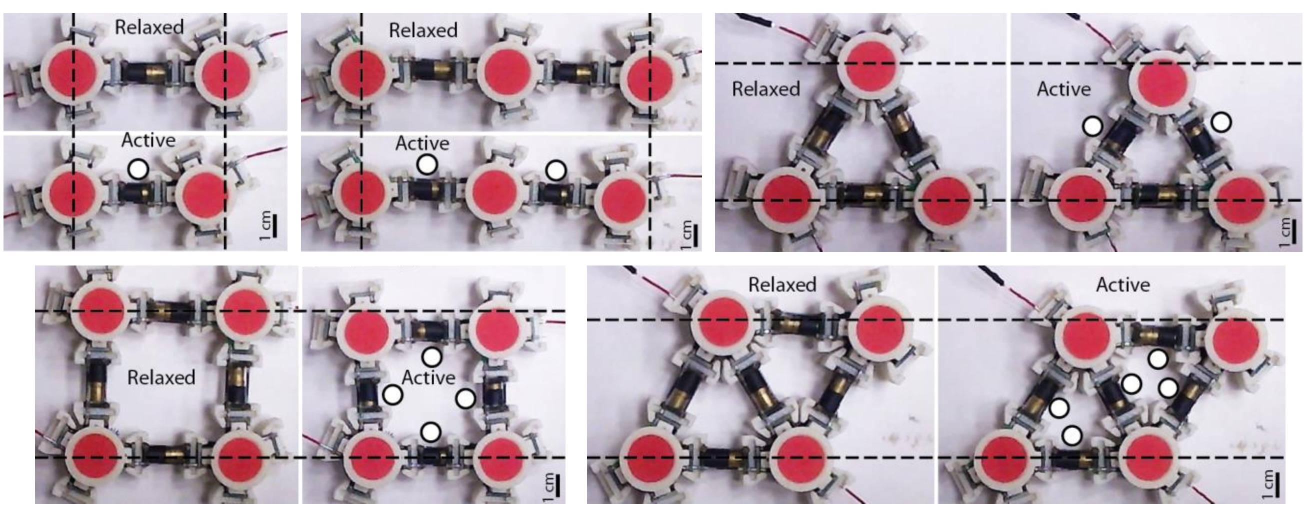

Figure 10 A set of prototype MACRO modules constructed using Active Cells and passive nodes (Nodes labeled with red circles for visual tracking). For each structure, the rest-shape as assembled and the deformed shape once the marked cells are activated is shown. Each structure was powered to drive 1.5A through the activated cells (marked), and no cooling system was used during testing. The figure shows a single cell (top row: left), two-cells in series (top row: middle), a triangle of three cells, (top row: right), a square of four cells (bottom row: left) and a set of two connected triangles (bottom row: right). Dashed guide-lines show MACRO deformations in the "Active" frame relative to the "Relaxed" frame in the relevant deformation direction.

described earlier) and multiple Active Cells along network edges.

An important question raised by these prototyped MACROs is that of controlled deformation of a given structure towards a specified target shape. This is a non-trivial problem and will be studied in our future work. In the same spirit, we intend to study the possibility of controlling network compliance by selectively actuating (and thus stiffening) local regions of the MACRO modules.

VI. Conclusions

We have demonstrated the feasibility of using Active Cells and associated nodes to design larger networks of deformable robotic structures (MACRO-modules). We have used our modeling of SMA coils to optimize the design of Active Cells. Using these cells and recently developed passive nodes, we have prototyped several small MACRO modules and demonstrated the possibility of creating compliant articulated robotic structures. While our studies on MACRO modules themselves are relatively preliminary, this work provides examples of potential modules that can be iteratively combined to create larger and more functional MACRO modules. We believe many interesting applications of these Active Cell-based structures can be explored in the future, including larger planar structures, spatial structures, and the investigation of algorithms to plan appropriate power control schemes to obtain a desired structural shape given any starting configuration of the robot.

References

[1] M. S. Moses and G. S. Chirikjian, "Simple components for a reconfigurable modular robotic system," in *2009 IEEE/RSJ International Conference on Intelligent Robots and Systems*, 2009, pp. 1478–1483.

[2] E. Hawkes, B. An, N. M. Benbernou, H. Tanaka, S. Kim, E. D. Demaine, D. Rus, and R. J. Wood, "Programmable matter by folding.," *Proc. Natl. Acad. Sci. U. S. A.*, vol. 107, no. 28, pp. 12441–12445, Jul. 2010.

[3] R. F. Shepherd, F. Ilievski, W. Choi, S. A. Morin, A. A. Stokes, A. D. Mazzeo, X. Chen, M. Wang, and G. M. Whitesides, "Multigait soft robot," *Proceedings of the National Academy of Sciences*, vol. 108, no. 51. pp. 20400–20403, Dec-2011.

[4] K. Gilpin, A. Knaian, and D. Rus, "Robot pebbles: One centimeter modules for programmable matter through self-disassembly," *Robot. Autom.*, pp. 2485–2492, May 2010.

[5] G. D. Hirst, "Mechanisms of peristalsis.," *Br. Med. Bull.*, vol. 35, no. 3, pp. 263–268, 1979.

[6] M. E. Silverman, D. Grove, and C. B. Upshaw, "Why does the heart beat? The discovery of the electrical system of the heart.," *Circulation*, vol. 113, no. 23, pp. 2775–81, Jun. 2006.

[7] M. Park, S. Chitta, A. Teichman, and M. Yim, "Automatic Configuration Recognition Methods in Modular Robots," *The International Journal of Robotics Research*, vol. 27, no. 3–4. pp. 403–421, 01-Mar-2008.

[8] J. Davey, N. Kwok, and M. Yim, "Emulating self-reconfigurable robots - design of the SMORES system," in *2012 IEEE/RSJ International Conference on Intelligent Robots and Systems*, 2012, pp. 4464–4469.

[9] T. Fukuda and T. Ueyama, *Cellular robotics and micro robotic systems*, vol. 10. World Scientific, 1994.

[10] M. Wooldridge, *An Introduction to MultiAgent Systems*. Wiley, 2009, p. 484.

[11] J. C. Barca and Y. A. Sekercioglu, "Swarm robotics reviewed," *Robotica*, vol. 31, no. 03, pp. 345–359, Jul. 2012.

[12] M. Yim, P. White, M. Park, and J. Sastra, "Modular Self-Reconfigurable Robots," in *Encyclopedia of Complexity and Systems Science*, 2009, pp. 19–33.

[13] M. Yim, W. W. Shen, B. Salemi, D. Rus, M. Moll, H. Lipson, E. Klavins, and G. Chirikjian, "Modular Self-Reconfigurable Robot Systems [Grand Challenges of Robotics]," *IEEE Robot. Autom. Mag.*, vol. 14, no. 1, pp. 43–52, Mar. 2007.

[14] E. Schweikardt and M. D. Gross, "Experiments in design synthesis when behavior is determined by shape," *Pers. Ubiquitous Comput.*, vol. 15, no. 2, pp. 123–132, Aug. 2010.

[15] D. Rus and M. Vona, "Crystalline Robots: Self-Reconfiguration with Compressible Unit Modules," *Auton. Robots*, vol. 10, no. 1, pp. 107–124, Jan. 2001.

[16] B. K. Wada, J. L. Fanson, and E. F. Crawley, "Adaptive Structures," *J. Intell. Mater. Syst. Struct.*, vol. 1, no. 2, pp. 157–174, Apr. 1990.

[17] P. C. Hughes, W. G. Sincarsin, and K. a. Carroll, "Trussarm--A Variable-Geometry-Truss Manipulator," *J. Intell. Mater. Syst. Struct.*, vol. 2, no. 2, pp. 148–160, Apr. 1991.

[18] L. Heller, D. Vokoun, P. Šittner, and H. Finckh, "3D flexible NiTi-braided elastomer composites for smart structure applications," *Smart Materials and Structures*, vol. 21, no. 4. p. 045016, 2012.

[19] Q. Luo and L. Tong, "Adaptive pressure-controlled cellular structures for shape morphing I: design and analysis," *Smart Mater. Struct.*, vol. 22, no. 5, p. 55014, 2013.

[20] J. P. Swensen and A. M. Dollar, "Active-Cells for the Construction of Redundant and Configurable Articulated Structures," in *Volume 1: Development and Characterization of Multifunctional Materials; Modeling, Simulation and Control of Adaptive Systems; Integrated System Design and Implementation*, 2013, p. V001T01A013.

[21] J. P. Swensen, A. I. Nawroj, P. E. I. Pounds, and A. M. Dollar, "Simple, scalable active cells for articulated robot structures," in *2014 IEEE International Conference on Robotics and Automation (ICRA)*, 2014, pp. 1241–1246.

[22] A. R. Pelton, V. Schroeder, M. R. Mitchell, X. Y. Gong, M. Barney, and S. W. Robertson, "Fatigue and durability of Nitinol stents," *J. Mech. Behav. Biomed. Mater.*, vol. 1, no. 2, pp. 153–164, Apr. 2008.

[23] S. Kim, E. Hawkes, K. Choy, M. Joldaz, J. Foleyz, and R. Wood, "Micro artificial muscle fiber using NiTi spring for soft robotics," in *2009 IEEE/RSJ International Conference on Intelligent Robots and Systems*, 2009, pp. 2228–2234.

[24] C. Pfeiffer, K. DeLaurentis, and C. Mavroidis, "Shape memory alloy actuated robot prostheses: initial experiments," *Proc. 1999 IEEE Int. Conf. Robot. Autom. (Cat. No.99CH36288C)*, vol. 3, pp. 2385–2391, 1999.

[25] K. Ikuta, M. Tsukamoto, and S. Hirose, "Shape memory alloy servo actuator system with electric resistance feedback and application for active endoscope," *Proceedings. 1988 IEEE Int. Conf. Robot. Autom.*, pp. 427–430, 1988.

[26] Y. Dong, Z. Boming, and L. Jun, "A changeable aerofoil actuated by shape memory alloy springs," *Mater. Sci. Eng. A*, vol. 485, no. 3010, pp. 243–250, 2008.

[27] K. J. Cho, E. Hawkes, C. Quinn, and R. J. Wood, "Design, fabrication and analysis of a body-caudal fin propulsion system for a microrobotic fish," *Proc. - IEEE Int. Conf. Robot. Autom.*, pp. 706–711, 2008.

[28] "Instron." [Online]. Available: http://www.instron.com/.

[29] S.-M. An, J. Ryu, M. Cho, and K.-J. Cho, "Engineering design framework for a shape memory alloy coil spring actuator using a static two-state model," *Smart Mater. Struct.*, vol. 21, no. 5, p. 055009, May 2012.

[30] I. Czarnocki, W. Kim, B. Utter, J. Luntz, D. Brei, and P. Alexander, "Design of SMA Helical Actuators: An Experimental Study," in *ASME 2013 Conference on Smart Materials, Adaptive Structures and Intelligent Systems*, 2013, pp. V001T04A017–V001T04A017.